

External Grant Award Number: 08HQGR0069 and 08HQGR0070

Submitted: December 2009

Title: Collaborative Research with California State Polytechnic University, Pomona, and URS Corporation: Rapid Estimates of Rupture Extent for Large Earthquakes Using Aftershocks

Authors:

Jascha Polet
Department of Geological Sciences
California State Polytechnic University
Pomona, CA 91768
Tel.: (909) 869-3459
E-mail: jpolet@csupomona.edu

Hong Kie Thio
URS corp
566 El Dorado Street, 2nd floor
Pasadena, CA 91101
Tel.: (626) 449-7650
E-mail: hong_kie_thio@urscorp.com

Abstract

We have developed an algorithm for the determination of first-order earthquake rupture parameters, such as fault length and azimuth, from the distribution of its immediate aftershocks with the purpose of extending the real-time analysis capabilities at the National Earthquake Information Center (NEIC).

The real-time availability of worldwide broadband waveform data has allowed seismologists to use sophisticated waveform techniques to rapidly study the source process of earthquakes, but the limitations of seismic waveform data and the complexities of the Earth's structure mean that the quick results from these methods may be of limited resolution. Using aftershock distributions to delineate the rupture plane and dimensions of the earthquake provides significant additional information on the earthquake rupture that could be important for rapid estimation of earthquake impact and useful as input for more sophisticated waveform techniques.

The close correlation between aftershocks and rupture extent has been used to estimate the fault dimensions of large historic earthquakes for which no, or insufficient, waveform data is available. We show that, in a near real-time earthquake monitoring environment, in which aftershocks of large earthquakes are routinely detected and located, these data may also be effective in determining a fast estimate of the first-order mainshock rupture parameters. To this end, we have developed an effective and fully automatic algorithm and have analyzed a large number of relatively recent large global and Southern California earthquakes and their aftershock sequences.

The algorithm automatically removes outliers by spatial binning, and subsequently determines the best fitting strike of the rupture and its length by projecting the aftershock epicenters onto a set of lines that cross the mainshock epicenter with incremental azimuths. For strike-slip or large dip-slip events, for which the surface projection of the rupture is rectilinear, the calculated strike correlates well with the strike of the fault and the corresponding length, determined from the width of the distribution of aftershocks projected onto the line, agrees well with the rupture length. In the case of a smaller dip-slip rupture with an aspect ratio closer to 1, the procedure gives a measure of the rupture extent and dimensions, but not necessarily the strike. We found that using standard earthquake catalogs, such as the National Earthquake Information Center and Southern California Seismic Network catalogs, we can constrain the rupture extent, rupture direction and strike of the mainshock using the aftershocks that occur within the first hour after the mainshock. In addition to their use in fast earthquake damage assessment, these rupture parameters would also provide useful input for further earthquake analyses, such as rupture modeling and Coulomb stress calculations. However, this aftershock data may not be currently available in near real-time. Since our results show that these early aftershock locations may be used to reliably estimate first order rupture parameters for large earthquakes, the near real-time availability of these data would be a valuable enhancement for fast earthquake analysis.

Introduction

The spatial distribution of aftershocks is closely linked to the rupture extent of the mainshock that preceded them. This correlation has frequently been used to estimate the fault dimensions of large historic earthquakes for which no, or insufficient, waveform data is available. With the advent of earthquake inversions that use seismic and geodetic data to constrain the slip distribution, the study of aftershocks has recently been largely focused on enhancing our understanding of the underlying mechanisms in a broader earthquake mechanics/dynamics framework.

However, in a real-time earthquake monitoring environment, in which aftershocks of large earthquakes are routinely detected and located, it may be very useful to use these data to determine a fast estimate of the first-order mainshock rupture parameters, which would aid in the rapid assessment of the impact of an earthquake (Earle and Wald, 2005) and which could help in constraining the input parameters of more sophisticated waveform inversions and Coulomb stress calculations. The goal of this project is to assess the feasibility of using aftershocks for the rapid evaluation of earthquake impact, develop a simple algorithm to this aim and define the input parameters needed for these calculations.

We have analyzed a number of large recent earthquakes and their aftershock sequences in an attempt to find an effective manner in which the rupture parameters of a mainshock can be deduced from its early aftershock distribution. We have focused our attention on earthquake sequences for which the rupture geometry has been determined independently. We have developed and applied a straightforward and fully automatic algorithm to these catalogs to determine the first-order characteristics of the aftershock distribution, such as the length and azimuth of the distribution, and compare them to the geometry and dimensions from slip models. Thus we show it is feasible to use aftershock locations to determine a rapid, first-order, estimate of the rupture parameters of a large earthquake, with the locations of aftershocks that occurred within the hour after the mainshock in the case of global earthquakes. This approach consequently provides the National Earthquake Information Center with an independent way to quickly estimate rupture extent.

A rapid assessment of aftershock distribution has become more feasible since recent improvements to the current monitoring systems, such as the introduction of the new HYDRA system operated by the NEIC (Benz et al., 2005) and the availability of real-time data. The use of aftershock data to estimate rupture area is an attractive option since this methodology would leverage existing data products, and therefore not add more complexity to the system.

General characteristics of aftershock sequences

In the following paragraphs we review the most common characteristics of aftershock sequences and their significance for the current study. Omori (1894) established that the rate of aftershocks from the 1891 Nobi (Mino-Owari) earthquake died off hyperbolically. He determined a hyperbolic relationship, now known as Omori's law, that describes this drop-off and was later modified by Utsu (1961) to the following form:

$$n(t) = \frac{K}{(t + c)^{-p}}$$

where t is time since mainshock, K and c are constants and power p is between 1 and 1.5 ($p=1$ in the original Omori law). The hyperbolic drop-off means that a large fraction of the aftershocks occurs in a relatively short time span after the mainshock, which is one of our motivations for using the immediate aftershocks to determine rupture extent.

The relationship between the spatial extent of aftershocks (S) and earthquake magnitude (M) was recognized by Utsu and Seki (1955), who found a relationship between the two that is not unlike more recent equations that relate magnitude and fault length (L):

$$\log S = M - 3.9$$

$$\log L = 0.5M - 1.8$$

These empirical relationships provide the main motivation for this project. They establish the general relationship between magnitude and aftershock zones. Using the aftershocks could therefore yield a quick independent magnitude estimate, although for real-time earthquake impact estimates, such as ShakeMap and PAGER, the extent of the rupture (length and azimuth) may be more immediately useful. The most commonly assumed mechanism for aftershock occurrence is the reorganization of the static stress field on the fault due to the mainshock occurrence (e.g. King et al., 1994) which is the reason why most aftershocks tend to occur at the edges of slip patches, or asperities, where the residual deviatoric stress is likely to have increased compared to the pre-earthquake state. This suggests that the initial distribution of aftershocks delineates the entire mainshock rupture zone and thus may be applicable in real-time environments. We will briefly discuss some issues with aftershock sequences extending beyond the rupture zone.

Spatio-temporal development of aftershock sequences

Aftershock sequences are not stationary in time, but instead evolve, often spreading beyond the immediate bounds of the mainshock rupture. Tajima and Kanamori (1985) carried out an extensive survey of spatio-temporal aftershock expansion patterns for large (subduction zone) earthquakes. Their main conclusions were that the difference between the 1-day and 1-year aftershock distributions varies widely between different types of earthquakes, with little expansion from the 1-day distribution for earthquakes with large asperities (“Chilean” type) compared to earthquakes with small asperities (“Marianas” type). The temporal expansion of aftershock zones beyond the initial rupture area is described as a diffusive process, and the actual mechanism may be related to rate and state dependent deformation (Dietrich, 1994), a cascading effect of multiple triggering of aftershocks (Helmstetter et al., 2003), viscous diffusion (Marsan and Bean, 2003; Mikuma and Miyatake, 1979) or post-seismic sliding (Kato, 2007). Most likely, the actual process involves all these mechanisms to a certain degree (Freed, 2005).

A characteristic of these diffusion processes, and the observed expansion rates, is that they occur over relatively long timescales and therefore are unlikely to be significant for the purpose of this study, which focuses on near real-time applications and thus relatively short time windows (a few hours at most) after the mainshock.

Triggered seismicity

We consider triggered seismicity to be different from the aftershocks that are directly related to the rupture. The triggering mechanism itself may be similar to the causative phenomenon that underlies aftershocks, such as changes in static stress, but may also include other mechanisms such shaking induced pore-pressure changes (Gomberg et al., 2001; Bosl and Nur, 2002; Yamashita, 2003). These triggered events pose a potential problem for the development of our algorithm. Whereas the diffuse aftershock expansion is unlikely to affect our results given the short time scales, the triggered events could cause us to over-estimate the rupture dimensions. In the case of the Landers and Hector Mine earthquakes, such triggered events occurred within a few hundred kilometers from the main rupture, and often in areas that were in the direction of the rupture propagation. Many occurred shortly after the mainshock. Therefore, we need to have a mechanism to discriminate these events from the “real” aftershocks. One of the goals of this study was to assess whether triggered seismicity poses a problem when trying to estimate a rupture area from the post-mainshock seismicity, and if so, what kind of criteria we can use to discriminate these events.

Method

The information required as input to our algorithm is limited to only an earthquake catalog, starting in time with the mainshock, as well as several fixed input parameters. For our

initial results, we used two different catalogs: the USGS/NEIC global earthquake catalog and the Southern California Seismic Network (SCSN) catalog, obtained from the Southern California Earthquake Center internet search interface. One of our goals was to determine how much time after the mainshock was required to be able to determine the rupture geometry from the epicentral locations of the aftershocks. For this study, we did not incorporate the depth of the events, since this is currently still a poorly resolved parameter in a global near real-time context. A follow-up study will explore the additional information on fault geometry that may be obtained with the use of depths as determined by local networks.

The algorithm contains the following steps, with the input parameters initially selected on the basis of trial-and-error and subsequently held fixed at the same values for all earthquakes. These steps are illustrated in Figure 1, using the example of the 1999 magnitude 7.1 strike-slip Hector Mine earthquake, located in the Mojave Desert region of Southern California.

- A geographical region is selected, based on the initial magnitude of the mainshock. The magnitude is used to determine an approximate fault length using the Wells and Coppersmith scaling relationships and the region of consideration is selected as a box with a width and height of 4 times this fault length, centered on the epicenter of the event. If the fault length determined by the algorithm turns out to be a significant portion of this width, the analysis is repeated for a box twice this initial size.
- To remove background seismicity and remotely triggered events and only consider true “aftershocks”, events with only a relatively small number of other nearby events are removed from the catalog (Figure 1a). The proximity cut-off is determined by catalog location accuracy, which is greater for a local catalog than a global catalog. After trial and error, we found that the optimal criterion used for the characterization of an earthquake as an aftershock was the presence of more than 5% of all events within 0.4° distance from its epicenter for the global, NEIC, catalog, or 0.2° in case of the local, SCSN, catalog.
- A projection of the aftershock epicenters is carried out onto straight lines centered on the mainshock epicenter, incremented by 15° in azimuth (Figure 1b).
- For each of these projected aftershock distributions, the length of this distribution is determined by moving out from the epicenter in steps of 5 km until 90% of aftershocks is contained (Figure 2a,b).
- The fault strike is then determined by selecting the azimuth of the line perpendicular to the most concentrated distribution, which may be defined in two possible ways (Figures 1c, 2c):
 1. the shortest projected distribution length or
 2. the distribution with the highest peak value

This approach has been determined to work well for moderate size to large strike slip earthquakes, as well as large dip-slip events, so earthquakes with a roughly rectangular rupture plane. The ratio between orthogonal (minimum/maximum) projection lengths is a measure of reliability of this strike estimate. For more square ruptures, an estimate can be obtained of rupture area. From the location of the mainshock epicenter within the aftershock distribution, the algorithm can also determine whether the mainshock rupture was bilateral or unilateral in nature.

Results and Conclusions

We show example results for the following global and California earthquakes in Figures 3 through 6.

- The 12 May 2008, Mw7.9 Sichuan, China, earthquake, with NEIC aftershock catalog
- The 26 January 2001, Mw7.6 Bhuj, India, earthquake, with NEIC aftershock catalog

- The 28 September 2004, Mw6.0 Parkfield, California, earthquake, with SCSN aftershock catalog
- The 26 December 2004, Mw9.1 Sumatra, Indonesia, earthquake, with NEIC aftershock catalog

The symbols, lines and notation in the figures and maps for these earthquakes are similar as those for the Hector Mine example earthquake (Figure 1).

A summary of our results for a selection of large global and California earthquakes is provided in Figures 3 through 6. The rupture length (Figure 7a,b) and, in the case of strike-slip earthquakes, the strike of the mainshock rupture are commonly accurately determined within one hour of the mainshock occurrence. The ratio between the determined rupture length and the width of the projected distribution of aftershocks orthogonal to it provides a measure of the reliability of the determined strike, with a high ratio indicating a more reliable strike result. Rupture lengths are generally well determined for California events using aftershocks in the local network catalog within 30 minutes of the mainshock, for the large global earthquakes using the NEIC aftershocks within one hour of the mainshock.

However, it is important to realize that this aftershock data likely is not available in near real-time, since the location of aftershocks is not a high priority for the SCSN and NEIC analysts in the first few hours after a large earthquake has occurred. This study shows that it would be a worthwhile endeavor to locate these events quickly, since these early aftershocks may provide significant constraints on the fault geometry of the mainshock, which is important for damage estimates and as input to more detailed seismic rupture and Coulomb stress analyses.

We are planning to expand upon this study to analyze all global events greater than magnitude 7 and all California events above 6.0 in the past decade and to investigate the improvement that might be possible by the inclusion of relocated depths from local networks. Although currently earthquake depths are not well constrained in real-time, it is likely that fast relative relocations will be determined in the near future by both global as well as local networks.

References

- Benz, H., Buland, R., Johnson, C., Bittenbinder, A. and Sipkin, 2007. HYDRA: NEIC's New Real-time Earthquake Response System. SSA 2005, Lake Tahoe, April 27-29.
- Bosl, W.J. and A. Nur, 2002. Aftershock and pore fluid diffusion following the 1992 Landers earthquake, *J. Geophys. Res.*, 107, 2366, doi:10.1029/2001JB000155.
- Das, S. and C. Henry, 2003. Spatial relation between main earthquake slip and its aftershock distribution, *Rev. of Geophys.*, 41, 3, doi:10.1029/2002RG000119.
- Earle, P. S., and D. J. Wald (2005). Helping Solve a Worldwide Problem— Rapidly Estimating the Impact of an Earthquake, USGS Fact Sheet, CPG Login 12/01/04
- Freed, A.M., 2005. Earthquake Triggering By Static, Dynamic, And Postseismic Stress Transfer, *Annu. Rev. Earth Planet. Sci.* 2005. 33:335–67
- Gomberg, J., P. A. Reasenberg, P. Bodin and R. A. Harris, 2001. Earthquake triggering by seismic waves following the Landers and Hector Mine earthquakes, *Nature* 411, 6836, doi:10.1038/35078053
- Helmstetter, A., G. Ouillon and D. Sornette, 2003. Are aftershocks of large Californian earthquakes diffusing? *J. Geophys. Res.*, 108, 2483, doi:10.1029/2003JB002503.
- Kato, N., 2007. Expansion of aftershock areas caused by propagating post-seismic sliding, *Geophys. J. Int.*, 168, 797-808.
- Mai, P.M., S. Jonsson, and F. Bethmann, SRCMOD - an online resource for finite-source rupture models of past earthquakes, SSA 2006, San Francisco, April 17-22, 2006.

- Marsan, D. and C.J. Bean, 2003. Seismicity response to stress perturbations, analysed for a world-wide catalogue, *Geophys. J. Int.*, 154, 179-195.
- Tajima, F. and H. Kanamori, 1985, Global survey of aftershock expansion patterns, *Phys. Earth Plan. Int.*, 40, 77-134.
- Utsu, T., 1961. A statistical study on the occurrence of aftershocks, *Geophys. Mag.*, **30**, 521–605.
- Utsu, T. and Seki, A., 1955. Relation between the area of aftershock region and the energy of the mainshock. *Zisin. 7*: 233–240.
- Yamashita, T., 2003. Regularity and complexity of aftershock occurrence due to mechanical interactions between fault slip and fluid flow, *Geophys. J. Int.*, 152, 20-33.

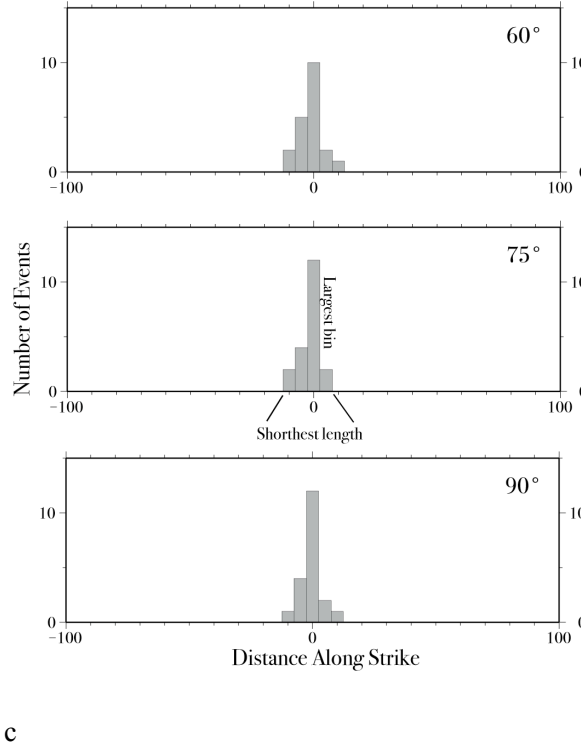
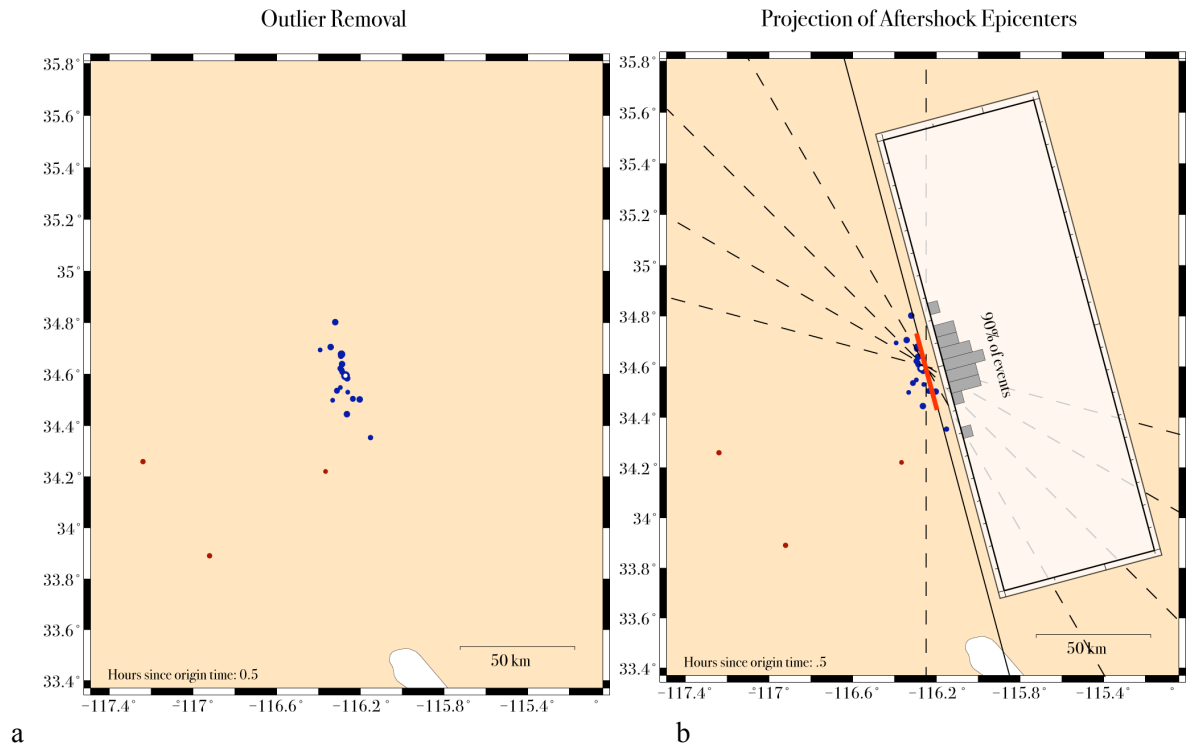


Figure 1. a - A map of the geographical region analyzed for the Hector Mine earthquake of 1999, using the standard (non-relocated) SCSN earthquake catalog. Blue events were classified as “aftershocks” by the algorithm, which considers as outliers (in red) those earthquakes that have fewer than 5% of the total number of events within 0.2° distance of its epicenter. **b** - The aftershocks are projected onto straight lines centered on the mainshock epicenters, separated by 15° in azimuth (not all lines are shown in this plot for clarity). These projected aftershock distributions are then binned in histograms with 5 km distance bins. Starting at the epicenter, the length of the projected distribution is determined by stepping outwards by 5 km steps, until 90% of the aftershocks is contained. **c** - The projected aftershock distributions for three different azimuths. For this earthquake, the azimuth with the shortest projected distribution length is 75° and two azimuths have the bin with the largest numbers of events: 75° and 90° .

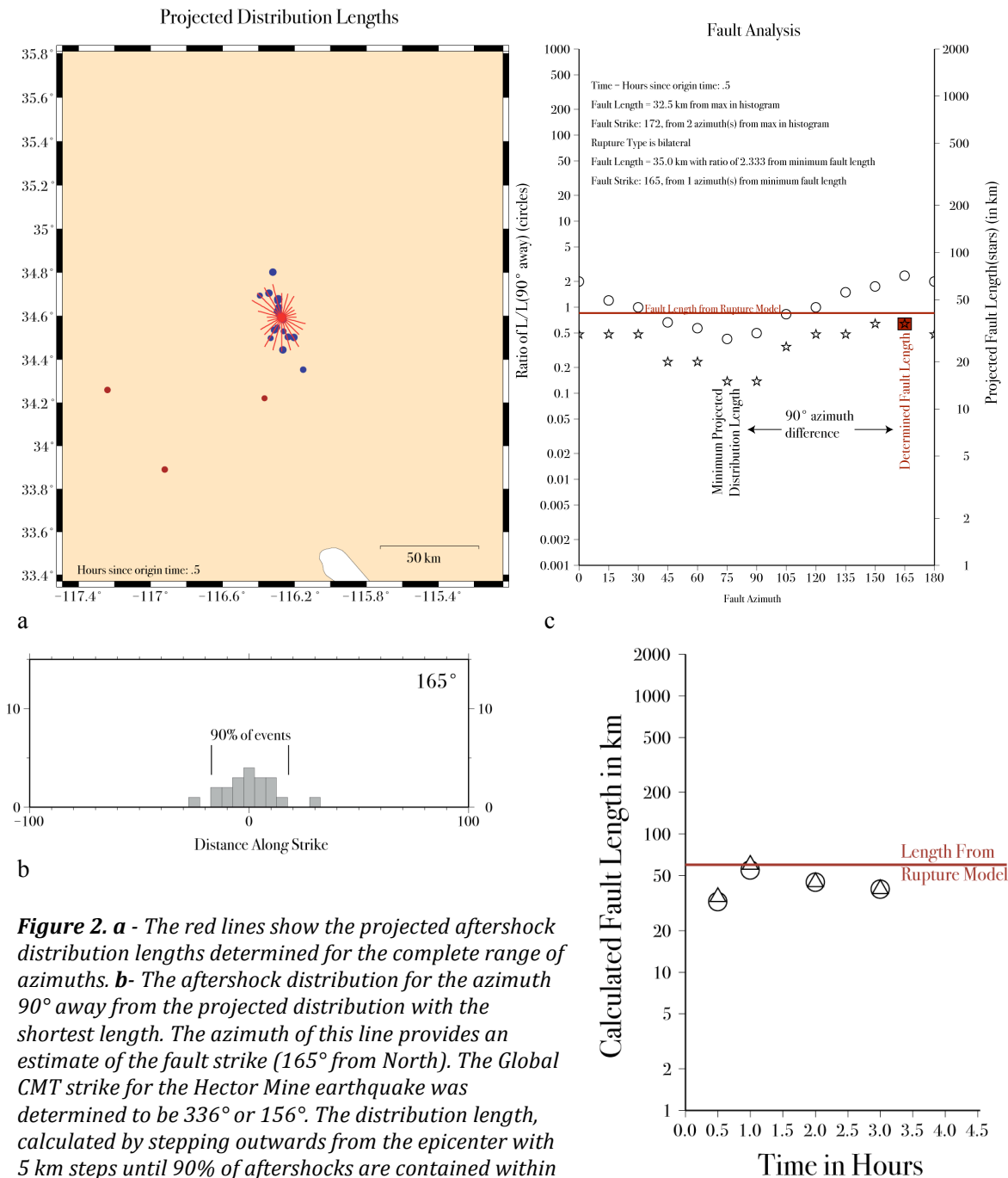


Figure 2. a - The red lines show the projected aftershock distribution lengths determined for the complete range of azimuths. **b** - The aftershock distribution for the azimuth 90° away from the projected distribution with the shortest length. The azimuth of this line provides an estimate of the fault strike (165° from North). The Global CMT strike for the Hector Mine earthquake was determined to be 336° or 156°. The distribution length, calculated by stepping outwards from the epicenter with 5 km steps until 90% of aftershocks are contained within the bounds of the interval, is determined to be 35 km and provides an estimate of rupture length. **c** - A summary of results for all azimuths, showing rupture lengths determined using the two different approaches. Assessment of the nature of the rupture (bilateral or unilateral) is based on the location of the epicenter relative to the determined rupture extent. When more than 75% of the rupture length estimate is located on one side of the epicenter, the rupture is categorized as unilateral. The ratio between the shortest distribution length and the length at an azimuth 90° away from this length determines how elongated the fault is, with better strike estimates determined for more elongated faults. **d** - The rupture length determined for the Hector Mine earthquake as a function of time of the aftershocks since the mainshock (as given by the local network catalog). A good estimate may be obtained after a half hour.

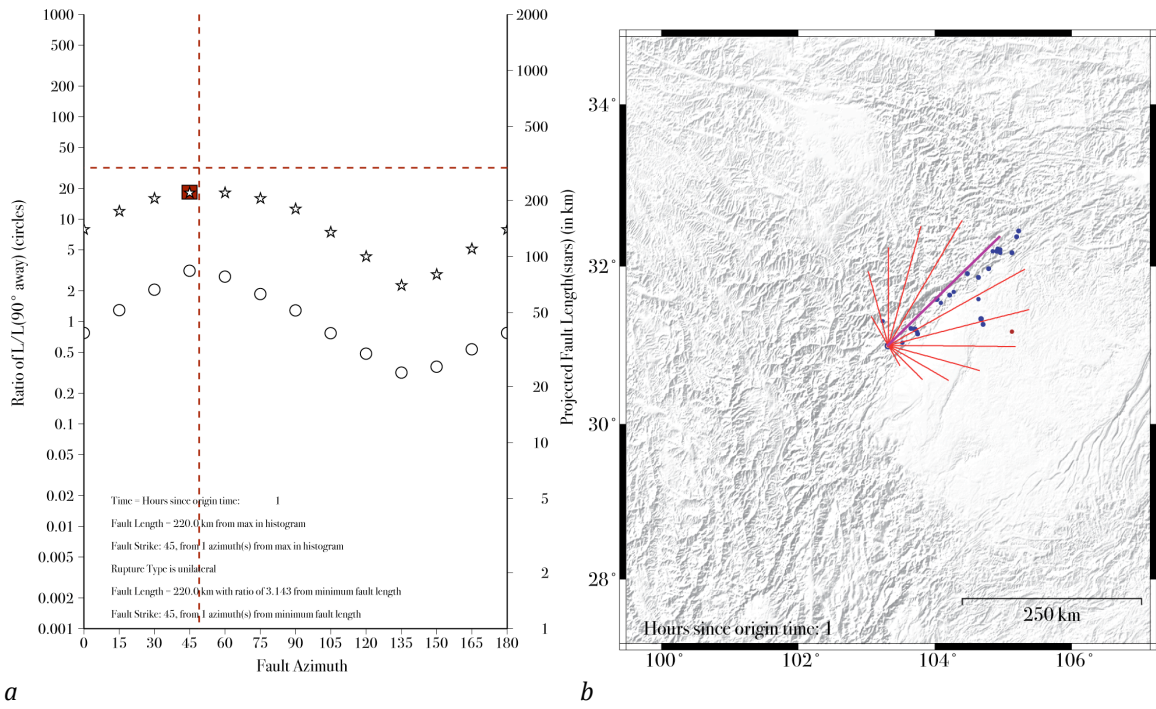


Figure 3. Results for the 2008 Wenchuan (Sichuan province) earthquake.

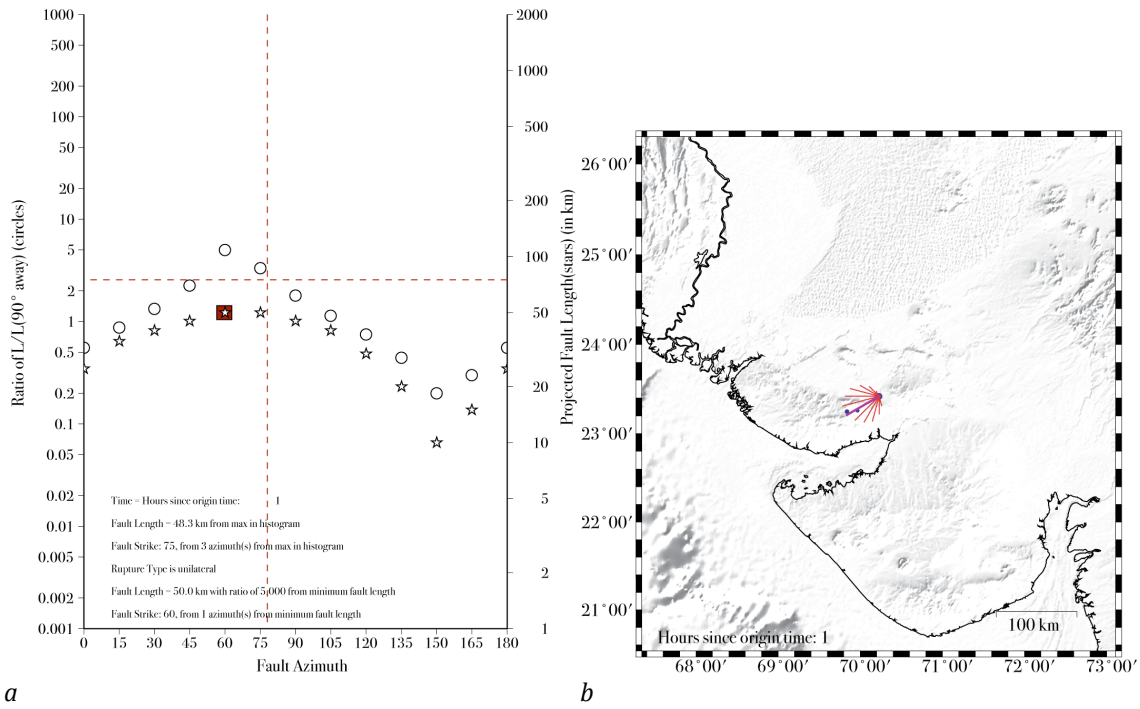


Figure 4. Results for the 2001 Bhuj, India, earthquake.

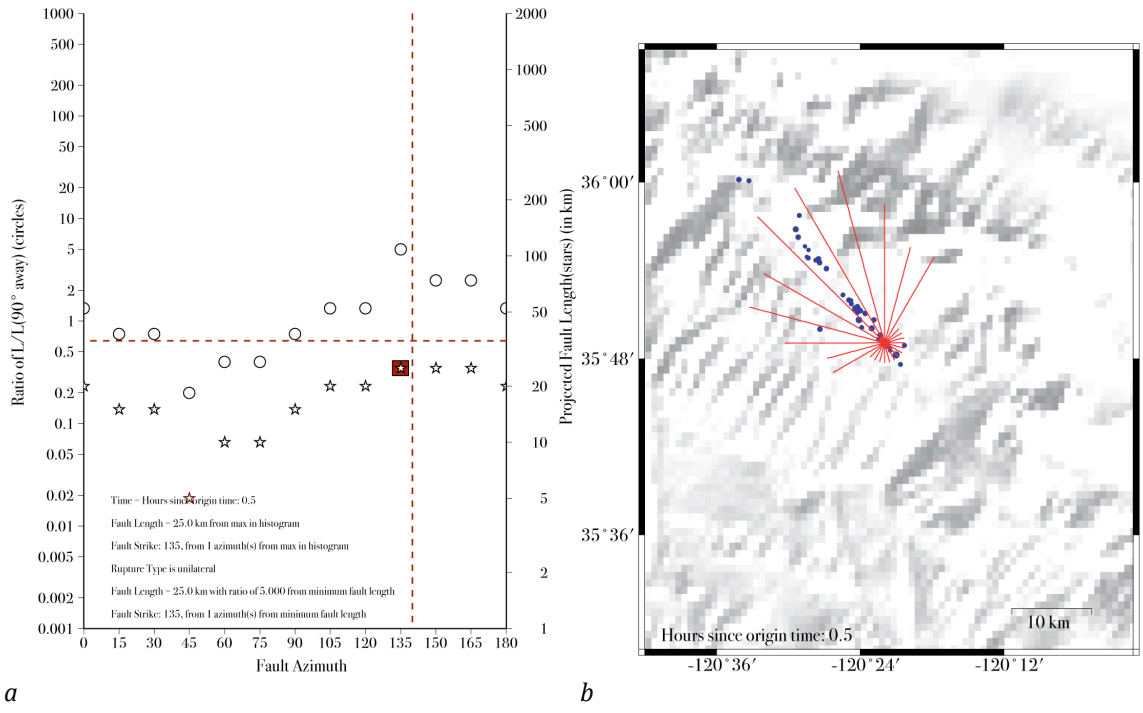


Figure 5. Results for the 2004 Parkfield earthquake

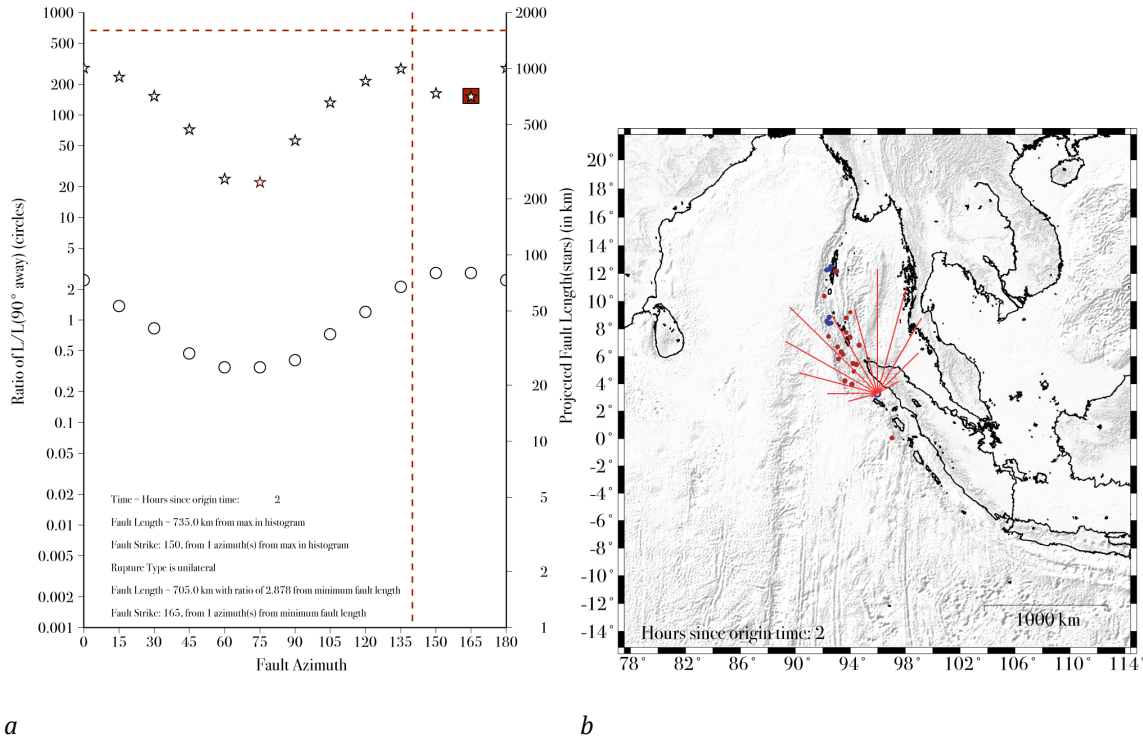
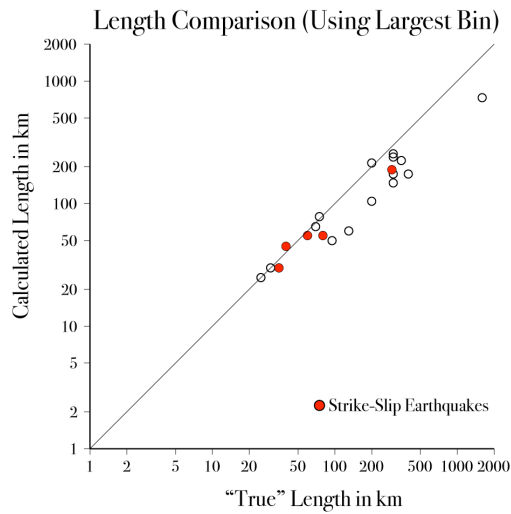
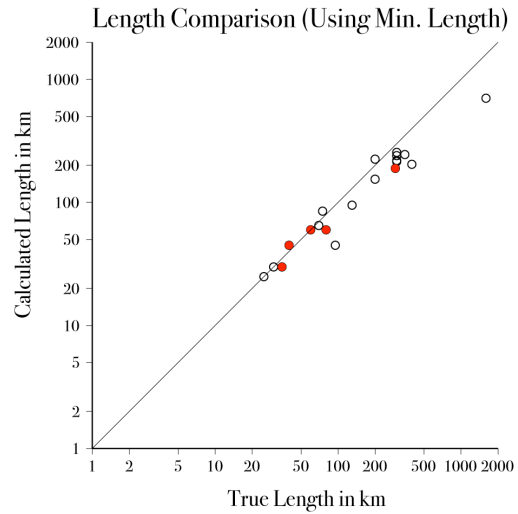


Figure 6. Results for the 2004 Sumatra earthquake.

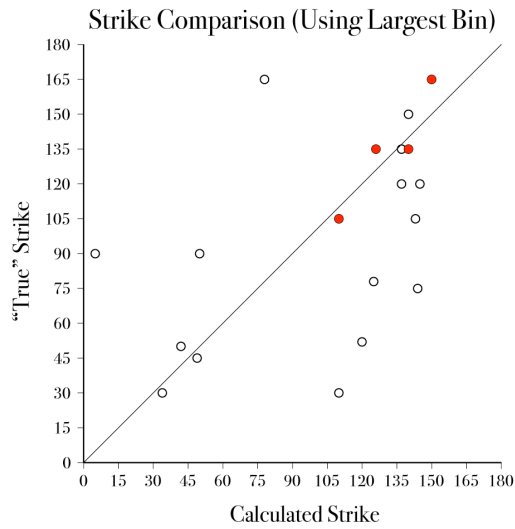


a

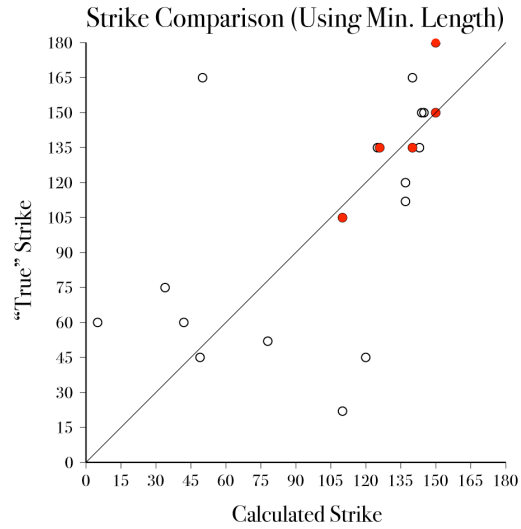


b

Figure 7. a - A comparison between the fault lengths determined using our algorithm for the largest bin of the projected aftershock distribution and length estimates determined from rupture models. **b** - Similar comparison, but for fault length measurements obtained using the minimum length approach.



a



b

Figure 8. a - A comparison between the strikes determined using our algorithm for the largest bin of the projected aftershock distribution and the Global CMT strike of the events. Strike values are accurately determined for earthquakes with elongated rupture planes: most strike-slip earthquakes and larger dip-slip events. **b** - Similar comparison, but for strike measurements obtained using the minimum length approach.